

Article

How the Presence of CO₂ Absorption Promoters and Composition of the Choline Chloride/Amine/Molecular Solvent Mixtures Influence Its Thermophysical Properties and Ability to Absorb Carbon Dioxide

Olga V. Kazarina ^{1,2,3,*} , Anna A. Golovacheva ^{2,3} , Zakhar A. Markin ³, Anton N. Petukhov ^{2,3} , Alexander S. Kazarin ³, Artem A. Atlaskin ² , Tatyana S. Sazanova ^{1,2} , Artyom N. Markov ³ , Alexander A. Kapinos ^{2,3}, Alexandra V. Barysheva ³, Sergey S. Suvorov ³, Egor S. Dokin ³ , Ilya V. Vorotyntsev ²  and Andrey V. Vorotyntsev ³ 

¹ Nizhny Novgorod State Technical University n.a. R.E. Alekseev, 24 Minina Street, 603950 Nizhny Novgorod, Russia

² Mendeleev University of Chemical Technology, 9 Miusskaya Square, 125047 Moscow, Russia

³ Chemical Engineering Laboratory, Research Institute for Chemistry, Lobachevsky State University of Nizhny Novgorod, Gagarina Avenue 23, 603950 Nizhny Novgorod, Russia

* Correspondence: olga_kazarina@list.ru



Citation: Kazarina, O.V.; Golovacheva, A.A.; Markin, Z.A.; Petukhov, A.N.; Kazarin, A.S.; Atlaskin, A.A.; Sazanova, T.S.; Markov, A.N.; Kapinos, A.A.; Barysheva, A.V.; et al. How the Presence of CO₂ Absorption Promoters and Composition of the Choline Chloride/Amine/Molecular Solvent Mixtures Influence Its Thermophysical Properties and Ability to Absorb Carbon Dioxide. *Environments* **2023**, *10*, 88. <https://doi.org/10.3390/environments10050088>

Academic Editors: William A. Anderson and Ching-Yuan Chang

Received: 6 April 2023

Revised: 6 May 2023

Accepted: 14 May 2023

Published: 18 May 2023



Copyright: © 2023 by the authors. Licensee MDPI, Basel, Switzerland. This article is an open access article distributed under the terms and conditions of the Creative Commons Attribution (CC BY) license (<https://creativecommons.org/licenses/by/4.0/>).

Abstract: The present research provides data on the density (ρ), viscosity (η) and ability to absorb carbon dioxide of systems containing amine, molecular solvent (MS) and choline chloride (ChCl), with the investigation of the physical properties of both neat amine/MS/ChCl mixtures and their samples after complete CO₂ saturation. The effect of the mixture composition was studied by varying amine from primary (monoethanolamine, MEA) to secondary (diethanolamine, DEA) and tertiary (triethanolamine, TEA) amine, and the degree of its substitution from a mono- (MEA, DEA and TEA) to a doubly-substituted (ethylenediamine, EDA) compound. The role of an MS was investigated via the exchange of ethylene glycol (EG) with water and dimethylsulfoxide (DMSO). In addition, the influence of the CO₂ absorption promoters present in the ternary MEA/EG/ChCl mixture at an amount of 5 wt. % was also investigated. We show that an increase in ρ and η in the amine/EG/ChCl mixture affects the properties of neat amines. This suggests that in the studied ternary mixtures, the nature of the interspecies interactions is very similar to those in the previously studied MEA/EG/ChCl system. When EG was exchanged for H₂O or DMSO, a decrease in ρ and an increase in η were observed. A comparison of the data with the corresponding properties of the systems composed of each pair of the mixture components indicates that the intensity and/or number of interspecies interactions in the present ternary mixtures were stronger than those in pure H₂O, DMSO and MEA. While in the presence of promoters no significant changes in the studied properties were found, for the corresponding CO₂-saturated samples, the ρ and η increased proportionally to the amount of absorbed gas. This was also the case for all the systems studied in the present research. The overall CO₂ absorption of the EG-based mixtures decreased when going from primary to secondary and tertiary amines; it was 21% higher for the MEA/H₂O/ChCl system compared to the mixtures containing EG and DMSO, which, in turn, showed similar absorption capacities. When the promoters were added to the MEA/EG/ChCl mixture, the highest capacity was found for the piperazine-containing system.

Keywords: amine-based mixtures; density; viscosity; carbon dioxide capture

1. Introduction

Even though novel ecological trends have stimulated the rapid development of renewable energy sources, energy supply remains widely dependent on carbonaceous fuels, especially fossil fuels such as crude oil, coal and natural gas [1]. Their incineration in mobile

power systems, power and industrial plants produces impressive amounts of greenhouse gas emissions, among which carbon dioxide is considered to be the most dangerous pollutant. An increase in its concentration in the atmosphere leads to global warming, and, as a consequence, to ocean acidification, the melting of glaciers, land desertification, and many other negative factors [2]. The Intergovernmental Panel on Climate Change has shown that 79% of carbon dioxide comes from burning fossil fuels that are used to generate electricity in coal-fired power plants, which are responsible for up to 60% of all CO₂ emissions [3].

Despite the intensive development of Carbon Capture and Storage (CCS) technologies aimed at reducing the negative impact of CO₂, its concentration in the atmosphere increased from 340 ppm in 1980 to 408 ppm in 2019 [4]. This means that the problem of the extraction of carbon dioxide from flue gas mixtures and its further processing will not lose its importance in the near future. The most common CCS techniques involve physical [5–10] and chemical [11–13] absorption, as well as low-temperature cryogenic [14,15] and membrane separation [14,16–18] processes. Among them, chemical absorption has been the most widely used and well-commercialized. It occupies a wide industry segment [19,20]; allows for the recycling of absorbents; enables temporary CO₂ fixing with further accumulation [21]; can be easily customized for favorable industrial process due to the diversity of compound structures [22]. When compared to alkali solutions, aqueous alkanolamines show lowered corrosion harm [23], and therefore have gained greater acceptance. Such primary amines as monoethanolamine (MEA) and 2-amino-2-methyl-1-propanol (AMP), secondary diethanolamine (DEA) and *di*-isopropanolamine (DIPA), tertiary *N*-methyl-diethanolamine (MDEA) and triethanolamine (TEA), and their blends, are the most widely considered systems for use in industrial CO₂ capture and storage [21,24,25]. With the advantages associated with high CO₂ solubility and a fast reaction rate, aqueous MEA still occupies the leading place in the market. However, MEA-based production lines have high energy demands during regeneration, lead to equipment corrosion caused by a high rate of solvent evaporation, and produce toxic compound emissions [26].

In whole or in part, these disadvantages can be overcome by an exchange of water via high-boiling point (HBP) solvents. Usually, the latter show a lower solvent heat capacity and evaporation enthalpy [27], as a result of which, when they are mixed with amines, HBP solvents contribute to significantly decreased amine evaporation and degradation, as well as equipment corrosion [26]. Moreover, it has been recently shown [28,29] that, because of their lower dielectric constant, a desorption process of MEA dissolved in HBP solvents can be facilitated due to the substantially reduced stability of the formed bicarbonate and carbamate. In addition, a significant improvement in the whole technology line can be achieved via the modification of amine CO₂ absorption (chemical method) in organic solvents via the physical methods of solvent regeneration, as shown, for example, in Ref. [30]. In principle, CO₂ absorption in HBP solutions has been carefully discussed for amines mixed with glycols [26,30–35] and glycol ethers [36], glycol/primary alcohol mixtures [27,30,34], propylene carbonate [31], *N*-methyl formamide [30], and *N*-methyl pyrrolidone (NMP) [34].

Due to their rather high liquid–gas transition temperatures, deep eutectic solvents (DESs) can be also considered as HBP solvents [37]. A diversity of possible combinations of starting materials, along with a hydrogen bond donor (HBD) and a hydrogen bond acceptor (HBA) in an appropriate molar ratio, provide powerful tools to control the properties of DESs and natural deep eutectic solvents (NADESs) [38] in accordance with their applications, including, among many others, pharmaceutical synthesis [39], band gap systems [40,41], and CO₂ capture [42–45]. Despite their absorption characteristics being inferior to conventional amine solutions, the systems in which DESs are mixed with amines or DESs comprising amines as HBDs are of particular interest when the optimization of the CO₂ absorption technology is considered. Surprisingly, a thorough literature search revealed only a few publications that provide a detailed study of the effect of the mixture of components, their ratio, the nature of amine, etc., on carbon dioxide capture by amine-based DESs and amine/DES mixtures [46–51].

In our previous work [52], we thoroughly investigated how the ratio of amine (MEA) to molecular solvent (EG) and electrolyte concentration (ChCl) in the MEA/EG/ChCl ternary system affects CO₂ absorption and such physical properties as density and viscosity. We showed that regardless of the components' ratio and temperature, a decrease in MEA content always results in a decrease in the solutions' absorption capacity (m_{CO_2}), expressed in moles of CO₂ absorbed by 1 kilo of a solution. Interestingly, ChCl seems to play no significant role in the CO₂ absorption process undertaken by the studied system. To check whether this is only the case for the previously studied MEA/EG/ChCl ternary system, or if this applies to all similar ternary systems containing amines and molecular solvents of different natures, the following steps were carried out. First, the compositions of the investigated systems were varied by switching from primary (MEA) to secondary (diethanolamine, DEA) and tertiary (triethanolamine, TEA) amines, and by varying the degree of amine substitution from mono- (MEA, DEA and TEA) to double-substituted amines (ethylenediamine, EDA). Second, the role of the molecular solvent was investigated via an exchange of a H-bonded EG with more polar water ($\epsilon_{20}^{\text{EG}} = 38.9$; $\epsilon_{20}^{\text{H}_2\text{O}} = 80.4$) and dimethylsulfoxide (DMSO), a solvent with a dielectric constant comparable to that of EG ($\epsilon_{20}^{\text{DMSO}} = 46.7$) but incapable of H-bonding. Finally, the MEA/EG/ChCl mixtures containing some substances recently found to act as CO₂ absorption promoters [53–56] were also studied. As a result, the thermophysical properties and CO₂ absorption characteristics of the amine/molecular solvent/ChCl (+additive) mixtures before and after complete CO₂ saturation have been carefully discussed.

2. Experimental Section

2.1. Materials

(2-Hydroxyethyl)-trimethylammonium chloride (choline chloride, ChCl; 99 wt. %) purchased from Acros Organics and 1,2-ethanediol (ethylene glycol, EG; >99 wt. %), propane-1,2,3-triol (glycerol, Gly; >99.6 wt. %), dimethyl sulfoxide (DMSO; >99.9 wt. %), and ammonium thiocyanate (NH₄SCN; >98 wt. %) supplied by Komponent Reaktiv (Moscow, Russia) were used without further purification. 2-Aminoethanol (monoethanolamine, MEA; >99.3 wt. %), bis-(2-hydroxyethyl)amine (diethanolamine, DEA; >99.2 wt. %), 1,2-diaminoethane (ethylenediamine, EDA; >99.5 wt. %), and tris-(2-hydroxyethyl)amine (triethanolamine, TEA; >99 wt. %) provided by «Oka-Sintez» Ltd. (Dzerzhinsk, Russia) were distilled under vacuum before use. The solvents were stored over freshly activated 3 Å molecular sieves in a desiccator filled with phosphorus pentoxide.

N,N,N',N'-tetramethylguanidine (TMG; >99 wt. %), 1,8-diazabicyclo[5.4.0]undec-7-ene (DBU; ≥99 wt. %) and 1,4-diazacyclohexane (piperazine, PP; >99 wt. %) were purchased from Sigma Aldrich.

Carbon dioxide (99.999 wt. %) and nitrogen (99.999 wt. %) were supplied by Monitoring (St. Petersburg, Russia); ammonia (99.99999 wt. %) was purchased from «Horst» Ltd. (Moscow, Russia). A brief overview of the substances used in this work is given in Table 1.

2.2. Mixture Preparation

In accordance with the findings obtained by us in Ref. [52] and briefly discussed in the Introduction, two series of ternary amine/molecular solvent/ChCl mixtures were prepared. The first series (I) comprised blends composed of amine (component 1), molecular solvent (component 2) and ChCl (component 3) with mole fractions (x_i)

$$x_i = \frac{m_i/M_i}{\sum m_i/M_i} \quad (1)$$

of $x_1 = 0.667$, $x_2 = 0.222$, and $x_3 = 0.111$, respectively. In Equation (1), m_i refers to the masses and M_i the molar masses of the mixture components. For the studied MEA/EG/ChCl system [52], this composition showed an optimal combination of absorbing capacity (m_{CO_2} , moles of CO₂ absorbed by 1 kg of a solution) and amine efficiency (c_{CO_2} , moles of CO₂ absorbed by 1 mole of amine). Due to this, the effect of the amine structure (primary,

secondary, or tertiary amine), the number of its NH_2 groups, and the influence of the molecular solvent substitution (see Table 2 for details) were investigated for mixtures with the above composition. Again, as was shown in [52], the best MEA efficiency (c_{CO_2}) for the MEA/EG/ChCl system was demonstrated in the mixture with $x_1 = 0.222$, $x_2 = 0.667$, and $x_3 = 0.111$. Thus, this mole fraction ratio (hereinafter called Series II) was used to figure out how the presence of additives (see Table 2) influences the c_{CO_2} values.

Accordingly, ternary mixtures of both compositions were prepared by weighing appropriate amounts of neat substances on an analytical balance with an accuracy of 0.1 mg. The mixtures were placed in tightly closed vials and, after complete mixing of the components, were stored over freshly activated 3 Å molecular sieves in a desiccator with P_2O_5 at room temperature. For the mixtures of Series II, the additives with mass fractions of 5% were added directly into the mixtures with Series II composition ($x_1 = 0.222$, $x_2 = 0.667$, $x_3 = 0.111$).

The composition of the mixtures investigated in the present work and their abbreviations, together with the structures of amines and additives comprising the systems of Series I and Series II, are given in Table 2. In order to simplify the interpretation of the used abbreviations, the latter consist of the series number (I for $x_1 = 0.667$ and II for $x_1 = 0.222$), the name of the amine and molecular solvent the mixtures are composed of for (Series I) and, additionally, the name of the additive (for Series II). For example, mixture I-MEA/EG comprises the MEA/EG/ChCl system with $x_{1=\text{MEA}} = 0.667$, $x_{2=\text{EG}} = 0.222$ and $x_{3=\text{ChCl}} = 0.111$, and mixture II-MEA/EG/TMG is the MEA/EG/ChCl system with $x_{1=\text{MEA}} = 0.222$, $x_{2=\text{EG}} = 0.667$ and $x_{3=\text{ChCl}} = 0.111$ containing 5 wt. % of TMG. Since all the prepared mixtures contain the same amount of ChCl ($x_3 = 0.111$), ChCl is omitted from all used abbreviations for the sake of simplicity.

To minimize the contact of the samples with air, preparatory operations were carried out in a flow of dry nitrogen. Additionally, the density (ρ), viscosity (η) and CO_2 absorption measuring cells were purged with N_2 prior to measurements with the sample transfer carried out using the syringe technique.

Water content, $w_{\text{H}_2\text{O}} = m_{\text{H}_2\text{O}}/m_{\text{sample}}$, expressed in parts per million (ppm), was estimated using the Karl Fischer titration (Metrohm 831 AG). The data on $w_{\text{H}_2\text{O}}$ for all the investigated samples are listed in Table S1.

2.3. Viscosity and Density Measurements

The Anton Paar SVM3001 instrument equipped with a Stabinger cell followed by a vibrating tube was used for dynamic viscosity (η) and density (ρ) measurements, carried out at atmospheric pressure. The instrument is characterized by a density repeatability of $0.00005 \text{ g}\cdot\text{cm}^{-3}$, a viscosity repeatability of 0.1%, and temperature stability of 0.005 K. Both the Stabinger viscosity and density measuring cells were calibrated using APS3, APN7.5, APN26, and APN415 calibration oils (Anton Paar, Austria) in accordance with the supplier calibration protocol. For density, a nominal measurement error of $u(\rho) = 0.05 \text{ g}\cdot\text{cm}^{-3}$ was estimated. Accordingly, the data collected in Tables S3 and S4 are given with the same number of digits. However, due to the limited purity of the samples [57], the expanded related uncertainty was found to be $U_r(\rho) = 0.001$ (confidence level 0.95). For viscosity, an expanded related uncertainty of $U_r(\eta) = 0.02$ (confidence level 0.95) was estimated.

The density and viscosity measurements were validated by comparing experimental data (Y^{exp}) and the fit (Y^{fit}) for APN7.5, APN26 and APN415 viscosity standards in terms of their deviations (δ)

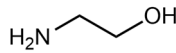
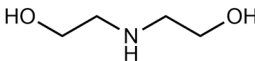
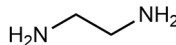
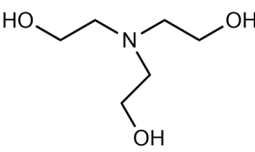
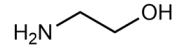
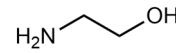
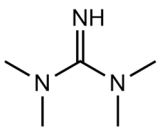
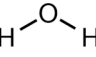
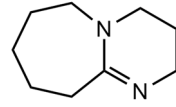
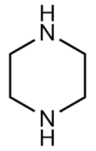
$$\delta = \frac{Y^{\text{exp}} - Y^{\text{fit}}}{Y^{\text{fit}}} \quad (2)$$

Table 1. Compound's chemical name, its CAS number, molar mass, supplier, initial mass fraction purity and water content, as well as the purification and drying procedures applied to the substances used in this work.

Chemical	CAS No.	Abbr.	Molar Mass ^a	Supplier	Mass Purity ^b	Initial Water Content ^{a,c}	Purification	Drying
2-aminoethanol	141-43-5	MEA	61.08	«Oka-Sintez» Ltd. (Dzerzhinsk, Russia)	>99.3	4000	Vacuum distillation	Activated 3 Å molecular sieves
bis-(2-hydroxyethyl)amine	111-42-2	DEA	105.14	«Oka-Sintez» Ltd. (Dzerzhinsk, Russia)	>99.2	4000	Vacuum distillation	
1,2-diaminoethane	107-15-3	EDA	60.10	Sigma Aldrich	>99.5	5000	Vacuum distillation	
tris-(2-hydroxyethyl)-amine	102-71-6	TEA	149.19	«Oka-Sintez» Ltd. (Dzerzhinsk, Russia)	>99.0	2000		
water	7732-18-5	H ₂ O	18.02	Millipore Milli-Q				
dimethyl sulfoxide	67-68-5	DMSO	78.13	Komponent Reaktiv (Moscow, Russia)	>99.9	1000	Recrystallization	
<i>N,N,N',N'</i> -tetramethyl-guanidine	80-70-6	TMG	115.18	Sigma Aldrich	>99.0	2000		
1,8-diazabicyclo[5.4.0]-undec-7-ene	6674-22-2	DBU	152.24	Sigma Aldrich	≥99.0	1500		
1,4-diazacyclohexane (2-hydroxyethyl)	110-85-0	PP	86.14	Sigma Aldrich	>99.0	1300	Recrystallization	
trimethylammonium chloride	67-48-1	ChCl	139.62	Acros Organics	99	6000		
1,2-ethanediol	107-21-1	EG	62.07	Komponent Reaktiv (Moscow, Russia)	>99.6	700		
ammonium thiocyanate	1762-95-4	NH ₄ SCN	76.12	Komponent Reaktiv (Moscow, Russia)	99	260	Recrystallization	Activated 3 Å molecular sieves
glycerol	56-81-5	Gly	92.09	Komponent Reaktiv (Moscow, Russia)	>99.6	600		Drying under reduced pressure
nitrogen	7727-37-9	N ₂	28.01	Monitoring (St. Petersburg, Russia)	99.9999			Activated 3 Å molecular sieves
carbon dioxide	124-38-9	CO ₂	44.01	Monitoring (St. Petersburg, Russia)	99.9999		Monitoring (St. Petersburg, Russia)	
ammonia	7664-41-7	NH ₃	17.03	Ltd. «Horst» (Moscow, Russia)	99.99999			

^a Units are g mol⁻¹ for molar mass and ppm for water content. ^b Provided by a supplier. ^c Mass fraction ($w_{\text{H}_2\text{O}} = m_{\text{H}_2\text{O}}/m_{\text{sample}}$), wt. %.

Table 2. Abbreviation and composition of the mixtures composed of amine (1), molecular solvent (2) and ChCl (3) with mole fractions of $x_1 = 0.667$, $x_2 = 0.222$, and $x_3 = 0.111$, respectively, (Series I) and with $x_1 = 0.222$, $x_2 = 0.667$, and $x_3 = 0.111$ with the presence of 5 wt. % of additives (Series II). Shown as well are amine and additive structures.

Series I: $x_1 = 0.667$, $x_2 = 0.222$, and $x_3 = 0.111$				
Mixture abbreviation	Amine	Amine structure		Molecular solvent
I-MEA/EG	MEA			EG
I-DEA/EG	DEA			EG
I-EDA/EG	EDA			EG
I-TEA/EG	TEA			EG
I-MEA/DMSO	MEA			DMSO
I-MEA/H2O	MEA			H2O
Series II: $x_1 = 0.222$, $x_2 = 0.667$, and $x_3 = 0.111$				
Mixture abbreviation	Amine	Molecular solvent	Additive name	Additive structure
II-MEA/EG	MEA	EG		
II-MEA/EG/TMG	MEA	EG	TMG	
II-MEA/EG/H2O	MEA	EG	H2O	
II-MEA/EG/DBU	MEA	EG	DBU	
II-MEA/EG/PP	MEA	EG	PP	

In the form of Y^{fit} values, the data provided by the supplier for the batches of oil, fitted with Equation (2) for density and Equation (3) for viscosity, were used for comparison. As seen in Figure S1, the deviations never exceeded the $-0.075 \leq 100\delta \leq +0.08$ interval for density and $-1.9 \leq 100\delta \leq +1.2$ for viscosity; that is, they were satisfactorily below the calculated expanded related uncertainties of $U_r(\rho) = 0.001$ and $U_r(\eta) = 0.02$, respectively.

For the obtained samples, density and viscosity as a function of temperature were recorded within the temperature range $T = (278.15\text{--}363.15)$ K with a step of 5 K. For the samples saturated with CO_2 at $T = 318.15$ K (see below), the measurements were carried out at atmospheric pressure and temperatures varying from 288.15 to 318.15 K. At higher temperatures, the measurements could not be performed due to partial gas release. In addition, for a number of samples, their viscosity $T < 293.15$ K was too high, which hampered ρ and η measurements at lower temperatures. We would here like to note that the $\rho(T)$ and $\eta(T)$ obtained for the CO_2 -saturated samples (Tables S4 and S6, respectively)

have been designed to show the general trend of the property change during the CO₂ absorption process, rather than to discuss and interpret their absolute values.

2.4. CO₂ Absorption Capacity

The CO₂ absorption capacity at $T = 313.15$ K was estimated as follows. A certain mass of solution (app. 10.0 g) was placed into a glass vial with an inner diameter of 12 mm and length of 200 mm, equipped with a cap with a long tube reaching the bottom of the vial (CO₂-input) and a CO₂-output tube with an electronic pressure sensor operating with an accuracy of 100 Pa. CO₂ was bubbled through the sample at a rate of $20 \text{ cm}^3 \cdot \text{min}^{-1}$ at $p = 0.1$ MPa (monitored by an electronic pressure sensor). During the measurements, the vial was thermostated in a T-3.1 water bath equipped with a precision temperature controller MIT-8.15 "Iztech" (Russia). The actual temperature was determined with a PTVS-4.2 KrioTherm thermocouple (Russia), $u(T) = 0.02$ K. During the measurements, the sample was mixed with a magnetic stirring bar. The mass gain during absorption was measured at regular intervals using a Shimadzu AUW220D electronic balance without buoyancy correction. Each solution was examined three times, and the average value of mass gain was taken for calculation. In order to take into account the weight loss associated with solvent evaporation, blank experiments consisting of bubbling of dry nitrogen through a sample were also carried out. The mixture absorption capacity (m_{CO_2}) and amine efficiency (c_{CO_2}) defined as the moles of CO₂ absorbed by 1 kg of a solution and by 1 mole of amine, respectively, were calculated from the maximum value of the mass gain. The mixtures obtained as such were further used for estimation of their density and viscosity.

In general, the reproducibility of CO₂ absorption measurements was within 0.5%. However, when the errors associated with the weighing, temperature, and mole fraction of the mixture components were taken into account, the associated uncertainty was found to be $U_r(m_{\text{CO}_2}) = 0.05$ for m_{CO_2} and $U_r(c_{\text{CO}_2}) = 0.05$ for c_{CO_2} .

The gas absorption measurements at $p = 0.1$ MPa were validated for 15 and 30 wt. % MEA solutions absorbing CO₂ at 298.15 and 313.15 K, and for a DES composed of NH₄SCN and glycerol in a molar ratio 2:3, absorbing NH₃ at 313.15 K. The reference values of their absorption capacity were taken from Refs. [58–63]. As seen in Table S2, the results obtained in the present work are in good agreement with the data derived by Huertas et al. [58], Deng et al. [59] and Li et al. [60], obtained gravimetrically, and in reasonable accordance with the volumetric measurements taken by Lee et al. [61], Jou et al. [62], and Shen and co-workers [63].

3. Results and Discussion

From a practical point of view, density and viscosity are fundamental properties whose temperature dependence must be considered when operating with fluids in any practical application. As mixtures containing amines (substances capable of capturing carbon dioxide) mixed with DES-like solvent are expected to have broad application in CCS technology, their physical properties are of particular interest for future use.

3.1. Density

The $\rho(T)$ data for the mixtures in Series I and II are listed in Table S3; Figure 1 displays the experimentally obtained $\rho(T)$ data (symbols) and their linear correlations (lines)

$$\rho = a_0 + a_1 T \quad (3)$$

where a_0 and a_1 are the fitting coefficients. The latter together with their standard deviations are listed in Table 3. The quality of the obtained experimental data was analyzed in terms of their deviations (δ , see Equation (2)) from the fit found with Equation (3). It has been shown that the δ values lie within the $-0.05 \leq 100\delta \leq +0.04$ range for mixtures of Series I and $-0.05 \leq 100\delta \leq +0.06$ for Series II. The fact that these deviations are substantially below the expanded related uncertainty of $U_r(\rho) \approx 0.001$ confirms the good quality of the obtained density data.

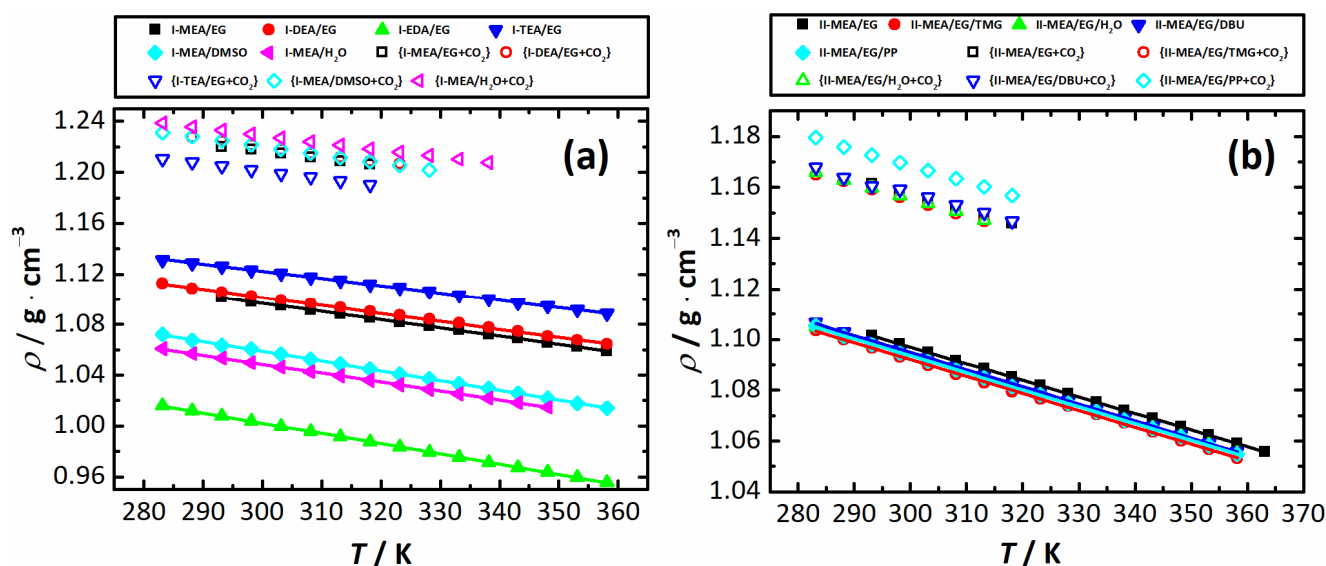


Figure 1. Densities (ρ) of neat (solid symbols) and CO_2 -saturated (open symbols) mixtures of Series I (a) and Series II (b) as a function of temperature (T). Lines are a result of the fit with Equation (3).

Table 3. Coefficients a_0 and a_1 and the associated fit standard error (σ_{fit}) obtained by fitting experimental $\rho(T)$ data with Equation (3).

System	a_0 ($\text{g} \cdot \text{cm}^{-3}$)	$10^4 a_1$ ($\text{g} \cdot \text{cm}^{-3} \cdot \text{K}^{-1}$)	$10^4 \sigma_{\text{fit}}$ ($\text{g} \cdot \text{cm}^{-3}$)	r^2
Series I: $x_1 = 0.667$, $x_2 = 0.222$, and $x_3 = 0.111$				
I-MEA/EG	1.2707 ± 0.0003	-6.995 ± 0.008	0.65	0.99994
I-DEA/EG	1.292 ± 0.002	-6.34 ± 0.05	1.32	0.99973
I-EDA/EG	1.2434 ± 0.0005	-8.04 ± 0.02	1.57	0.99994
I-TEA/EG	1.2892 ± 0.0009	-7.68 ± 0.03	2.56	0.99982
I-MEA/DMSO	1.2594 ± 0.0003	-7.03 ± 0.01	0.78	0.99998
I-MEA/ H_2O	1.2944 ± 0.0009	-5.74 ± 0.03	2.59	0.99967
Series II: $x_1 = 0.222$, $x_2 = 0.667$, and $x_3 = 0.111 + 5$ wt. % of additive				
II-MEA/EG	1.2927 ± 0.0002	-6.524 ± 0.007	0.57	0.99994
II-MEA/EG/TMG	1.291 ± 0.001	-6.63 ± 0.04	3.55	0.99953
II-MEA/EG/ H_2O	1.2903 ± 0.0002	-6.549 ± 0.007	0.68	0.99998
II-MEA/EG/DBU	1.2966 ± 0.0005	-6.73 ± 0.01	1.35	0.99993
II-MEA/EG/PP	1.2931 ± 0.0007	-6.65 ± 0.02	2.15	0.99983

As seen in Figure 1a, the exchange of amine and molecular solvent components significantly affects the density of Series I mixtures. For systems with varying component 1, this effect is in conformity with the density of neat amines. Its increase observed in the order EDA ($\rho_{\text{EDA}}^{303.15} = 1.25640 \text{ g} \cdot \text{cm}^{-3}$) < MEA ($\rho_{\text{MEA}}^{303.15} = 1.00809 \text{ g} \cdot \text{cm}^{-3}$) < DEA ($\rho_{\text{DEA}}^{303.15} = 1.08813 \text{ g} \cdot \text{cm}^{-3}$) < TEA ($\rho_{\text{TEA}}^{303.15} = 1.11847 \text{ g} \cdot \text{cm}^{-3}$) is reflected in the density of their ternary mixtures, that is, I-EDA/EG < I-MEA/EG < I-DEA/EG < I-TEA/EG. As was shown in Ref. [52], ChCl has a structure-breaking effect on the mixed MEA/EG solvent, in which packing effects dominate over H-bonding interactions. The above order of the systems' density allows one to suggest that in ternary mixtures comprising amine, EG and ChCl, the nature of the interspecies interactions is very similar to that of those in the previously studied MEA/EG/ChCl system.

When the molecular solvent (EG) is exchanged for H_2O or DMSO, a decrease in density is observed. For the mixture containing water as a molecular solvent, the density increases from $\rho_{\text{H}_2\text{O}}^{298.15} = 0.99704 \text{ g} \cdot \text{cm}^{-3}$ for pure water to $\rho_{\text{I-MEA/H}_2\text{O}}^{298.15} = 1.04982 \text{ g} \cdot \text{cm}^{-3}$ for I-MEA/ H_2O . A literature search shows that this behavior is typical for binary mixtures

composed of ChCl and MEA (or H₂O). For example, aqueous solutions of both ChCl [64] and MEA [65] within an entire solubility range have densities higher than that of pure water. When dissolved in MEA, ChCl also increases the density of the obtained solutions, as shown in Ref. [66]. Thus, the MEA/ChCl/H₂O mixture displays an intuitively expected trend of density increase. However, one cannot say that each mixture component has a positive impact on the observed property change, as density only reflects an overall effect governed by the ion–ion, ion–molecule and molecule–molecule interactions present in a ternary system comprising an electrolyte (ChCl). As a result, in order to figure out the individual contribution of each of the mixture's components and/or the above interactions, a more detailed investigation, including a property scan by component content at a constant ratio of the other two components, should be performed.

Although we did not find any support in the literature, it is very likely that, similar to many electrolyte systems, the addition of ChCl to DMSO leads to a density increase. Apparently, an assumed positive effect of ChCl on the DMSO density and the confirmed positive impact on MEA density [66] are compensated by a negative MEA–DMSO contribution in the mixture I-MEA/DMSO. Its density, equal to $\rho_{\text{I-MEA/DMSO}}^{298.15} = 1.06345 \text{ g}\cdot\text{cm}^{-3}$, is lower than of pure solvent, $\rho_{\text{DMSO}}^{298.15} = 1.09519 \text{ g}\cdot\text{cm}^{-3}$ [67]. As shown in Ref. [68], an increase in MEA content in the MEA/DMSO system leads to a decrease in its density, which is mainly caused by packing effects (excess molar volume increases with increasing temperature). Therefore, the density of the mixture I-MEA/DMSO is affected by the strength and flexibility of the network formed in a mixed MEA/DMSO solvent. For Series II mixtures (see Figure 1b), no significant density changes are observed. In the presence of all the additives used, the ρ slightly decreases compared to the II-MEA/EG system.

The density values of the CO₂-saturated samples collected in Table S4 are always higher than those for initial mixtures. Its increase is caused by the formation of products of the reaction between amine and carbon dioxide. When discussing Series I mixtures, the density of the CO₂-saturated samples is in very good agreement with the amount of the absorbed gas (see below), that is, it increases more when going from I-TEA/EG to I-MEA/H₂O than when going to I-MEA/DMSO \approx I-MEA/EG and I-DEA/EG, and, finally, to I-EDA/EG. As seen in Figure 1a, for the density of CO₂-saturated samples of Series I, the sequence is I-TEA/EG < I-MEA/EG < I-DEA/EG \approx I-MEA/DMSO < I-MEA/H₂O. We here note that during the course of CO₂ absorption by the I-EDA/EG mixture, a precipitate is formed and, as a result, the mixture completely solidifies. Due to this, no density was measured for it.

Apparently, the situation is very similar when Series II mixtures studied after complete CO₂ saturation are considered. Here, among the CO₂-saturated samples, the highest density is observed for II-MEA/EG/PP, that is, again, for the sample showing the highest absorption capacity, m_{CO_2} . However, since for the mixtures containing other additives (TMG, DBU, and H₂O) their ρ_{CO_2} values are very close to that of the neat II-MEA/EG system, their density values appear to be very close to each other.

3.2. Viscosity

The logarithmic viscosities (η) of neat and CO₂-saturated mixtures of Series I and II estimated within the temperature range of $T = (283.15 \text{ to } 353.15) \text{ K}$ are shown in Figure 2a,b; the corresponding viscosity values are summarized in Tables S5 and S6, respectively. Experimental $\ln \eta$ values for Series I and Series II as a function of temperature (T) were fitted using the Vogel–Fulcher–Tammann (VFT) equation

$$\ln \frac{\eta}{\eta_0} = \ln \left(\frac{A_\eta}{\eta_0} \right) + \frac{B_\eta}{T - T_{0,\eta}} \quad (4)$$

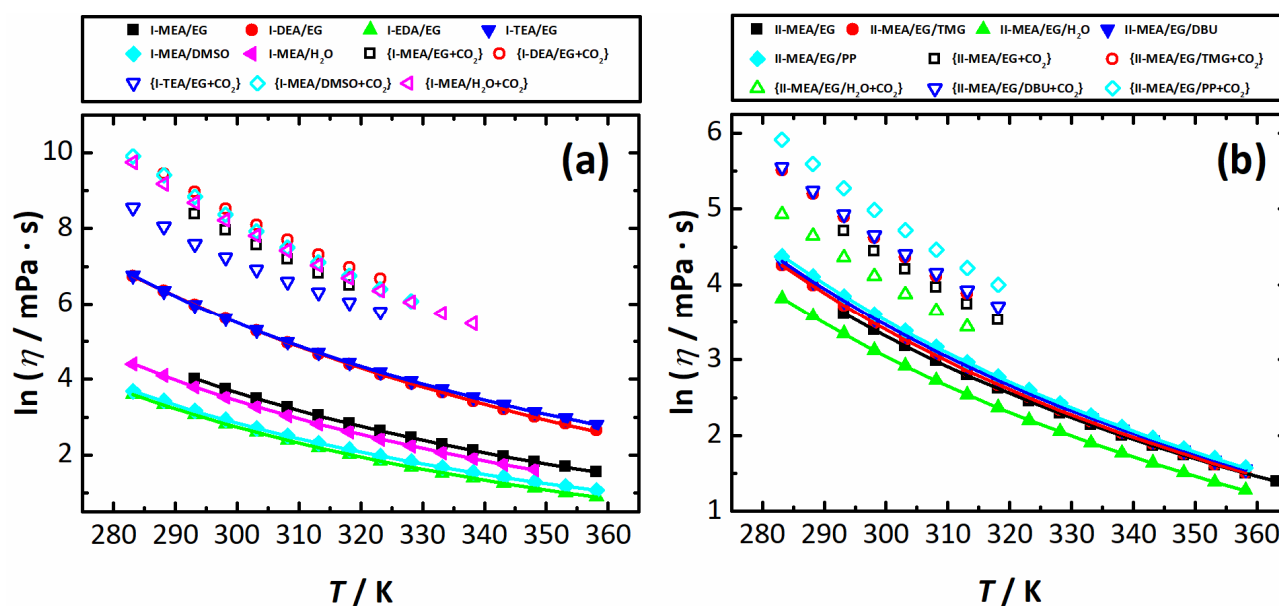


Figure 2. Logarithmic viscosities ($\ln \eta$) of neat (solid symbols) and CO_2 -saturated (open symbols) mixtures of Series I (a) and Series II (b) as a function of temperature (T). The lines are a result of the fit with Equation (4).

In Equation (3), $\eta_0 = 1 \text{ mPa} \cdot \text{s}$, A_η is the viscosity limit at an infinite temperature, B_η is the coefficient linked by relation with the pseudo activation energy, and $T_{0,\eta}$ is the VFT temperature. The parameters of Equation (4) are summarized in Table 4.

Table 4. Coefficients A_η , B_η , and $T_{0,\eta}$; the associated fit standard error (σ_{fit}) obtained by fitting experimental $\eta(T)$ data with Equation (4).

x_2	$\ln A_\eta/\eta_0$	$B_\eta(\text{K})$	$T_{0,\eta}(\text{K})$	$10^3 \sigma_{\text{fit}}$	r^2
Series I: $x_1 = 0.667$, $x_2 = 0.222$, and $x_3 = 0.111 + 5 \text{ wt. } \%$					
I-MEA/EG	-3.53 ± 0.05	1012 ± 17	159 ± 1	2.96	0.99989
I-DEA/EG	-4.9 ± 0.1	1590 ± 36	146 ± 2	6.77	0.99998
I-EDA/EG	-3.43 ± 0.07	839 ± 21	164 ± 2	5.55	0.99996
I-TEA/EG	-2.99 ± 0.06	775 ± 18	167 ± 2	5.05	0.99997
I-MEA/DMSO	-3.69 ± 0.07	1000 ± 21	160 ± 2	3.88	0.99998
I-MEA/ H_2O	-3.58 ± 0.04	1249 ± 13	162 ± 1	3.21	0.99999
Series II: $x_1 = 0.222$, $x_2 = 0.667$, and $x_3 = 0.111 + 5 \text{ wt. } \%$ of additive					
II-MEA/EG	-3.40 ± 0.08	1057 ± 30	142 ± 3	3.87	0.99997
II-MEA/EG/TMG	-3.41 ± 0.09	1026 ± 31	149 ± 2	6.03	0.99996
II-MEA/EG/ H_2O	-3.64 ± 0.08	1078 ± 28	139 ± 2	4.64	0.99997
II-MEA/EG/DBU	-3.60 ± 0.04	1105 ± 14	144 ± 1	2.49	0.99999
II-MEA/EG/PP	-3.83 ± 0.05	1183 ± 19	139 ± 1	3.08	0.99999

For all of the experimental points, the deviation from the fit does not exceed the limits of $-0.95 \leq 100\delta \leq +0.76$ for Series I systems, and lies within the interval of $-0.47 \leq 100\delta \leq +0.49$ for Series II mixtures. Thus, these deviations are lower than the expanded related uncertainty estimated for viscosity, $U_r(\eta) = 0.02$.

Similar to density, the viscosity of the Series I systems containing EG as a molecular solvent correlate well with the viscosities of the neat amines used for the mixture preparation. For amines, the viscosity increases in the pattern EDA ($\eta_{\text{EDA}}^{303.15} = 1.26 \text{ mPa} \cdot \text{s}$) < MEA ($\eta_{\text{MEA}}^{303.15} = 14.9 \text{ mPa} \cdot \text{s}$) < DEA ($\eta_{\text{DEA}}^{303.15} = 389 \text{ mPa} \cdot \text{s}$) \approx TEA ($\eta_{\text{TEA}}^{303.15} = 405 \text{ mPa} \cdot \text{s}$). As seen in Figure 2a, within the entire temperature range, I-DEA/EG and I-TEA/EG have the highest viscosity in comparison with the reference I-MEA/EG system, while I-EDA/EG exhibits

a viscosity lower than I-MEA/EG. Similarly, molecular solvent substitution has a very pronounced effect on the systems' viscosity. For both I-MEA/H₂O and I-MEA/DMSO, a viscosity increase is observed compared to pure molecular solvents, i.e., from 0.890 mPa·s for H₂O to 277 mPa·s for I-MEA/H₂O, and from 2.06 mPa·s for DMSO to 34.1 mPa·s for I-MEA/DMSO at 298.15 K. Obviously, for both systems, their viscosity is higher than that of MEA, $\eta_{\text{MEA}}^{298.15} = 18.7$ mPa·s. This indicates that the intensity and/or number of interspecies interactions (presumably H-bonds) in the studied ternary mixtures are stronger than the MEA–MEA, H₂O–H₂O and DMSO–DMSO interactions in pure solvents. In addition, a possible positive contribution of the ChCl molecular solvent (alternatively, the Ch⁺/Cl[−]-molecular solvent) interaction to the systems' viscosity cannot be ruled out. However, without the additional investigation of the H-bonds present in the above systems using spectroscopic techniques able to probe the discussed interactions, the above should be taken with a grain of salt.

Obviously, due to facilitated mass transport, systems exhibiting low viscosity are of particular interest when gas absorption processes are considered. Thus, an exchange of EG ($\eta_{\text{I-MEA/EG}}^{298.15} = 42.3$ mPa·s) or water ($\eta_{\text{I-MEA/H}_2\text{O}}^{298.15} = 42.3$ mPa·s) in their absorbing mixtures for DMSO seems to be a solution to decreasing the system's viscosity. However, as clearly seen in Figure 2a, a saturation of the corresponding sample by CO₂ leads to a significant viscosity increase, which definitely decreases the rate of the absorption process (see discussions below). As seen in Figure 2a and Table S5, the system I-EDA/EG has the lowest viscosity of $\eta_{\text{I-EDA/EG}}^{298.15} = 16.8$ mPa·s among the systems of Series I, which also makes it quite a promising mixture for efficient CO₂ absorption. Unfortunately, again, it can be hardly considered for this purpose as, during the course of the gas purge, a precipitate is formed, which results in the complete solidification of the sample.

The addition of TMG, DBU and PP has rather slight positive effects (viscosity increase) on II-MEA/EG; see Figure 2b. For water, the more pronounced negative effect can be explained by H₂O's small molar mass and, as a result, higher concentration when a mass fraction of 5% is converted to a mole fraction, which means that the relation of H₂O to other mixture constituents is significantly greater than in II-MEA/EG/PP, II-MEA/EG/DBU and II-MEA/EG/TMG. Although the viscosity of Series II mixtures is rather hard to interpret, for the corresponding CO₂-saturated samples, $\eta(T)$ is in full agreement with the amount of absorbed CO₂. As seen in Figure 2b, viscosity decreases in the order II-MEA/EG/PP > II-MEA/EG/DBU \approx II-MEA/EG/TMG > II-MEA/EG > II-MEA/EG/H₂O, that is, in the exact same order as the absorption capacities of the Series II mixtures (see Table S7).

3.3. CO₂ Absorption

The potential of the chosen systems for use as CO₂ absorption agents was analyzed in terms of their absorbing capacities (m_{CO_2}) and amine efficiencies (c_{CO_2}), estimated from the absorption profiles shown in Figures 3a and 4a. As seen, the overall CO₂ absorption of the EG-based mixtures decreases from I-MEA/EG to I-DEA/EG and I-TEA/EG, demonstrating a decrease in the CO₂ absorption when going from primary to secondary and tertiary amines, respectively. This tendency is quite common, and reflected in the literature, such as in Refs. [69–71]. For the above systems, m_{CO_2} achieves approximately 95% of its maximum in 30 min. The same level of saturation (but reached faster) is observed for I-MEA/DMSO and I-MEA/H₂O, i.e., the systems in which EG is exchanged for DMSO and H₂O, respectively. The rise in the absorption rate, shown in Figure 3b for systems of Series I, for I-MEA/DMSO and I-EDA/EG is definitely caused by their lower viscosity compared to I-MEA/EG (see discussions above).

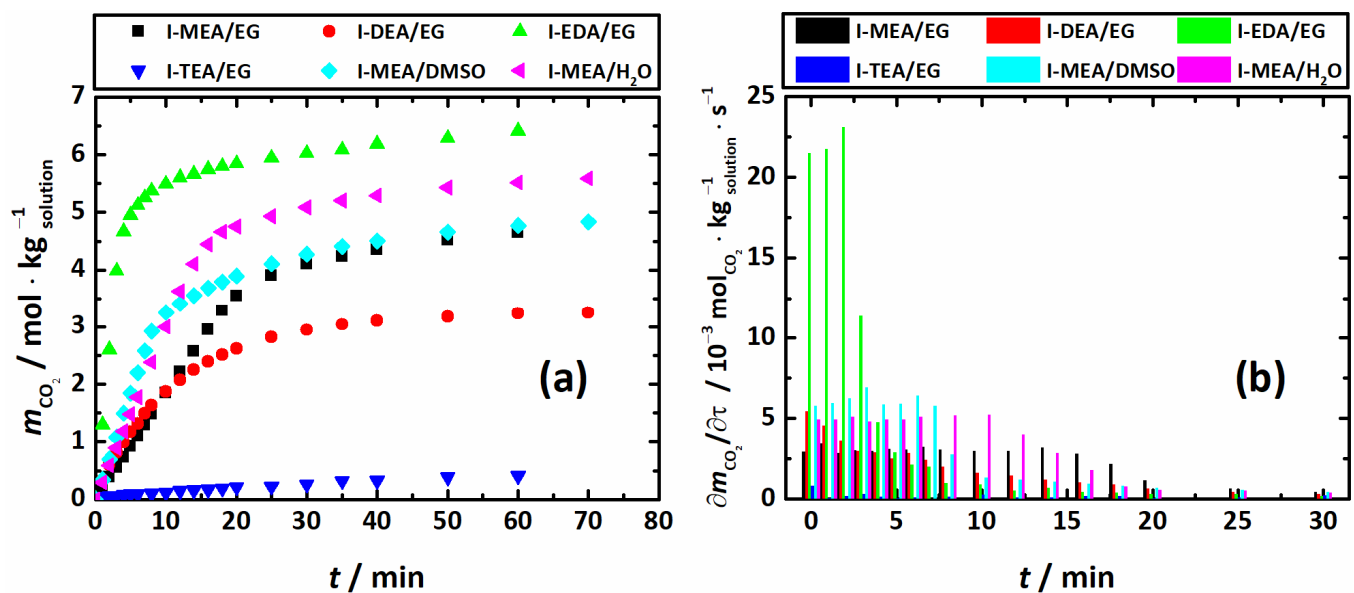


Figure 3. Absorption profiles (a) and absorption rates ($\partial m_{\text{CO}_2} / \partial \tau$) (b) of Series I systems, $T = 313.15$ K.

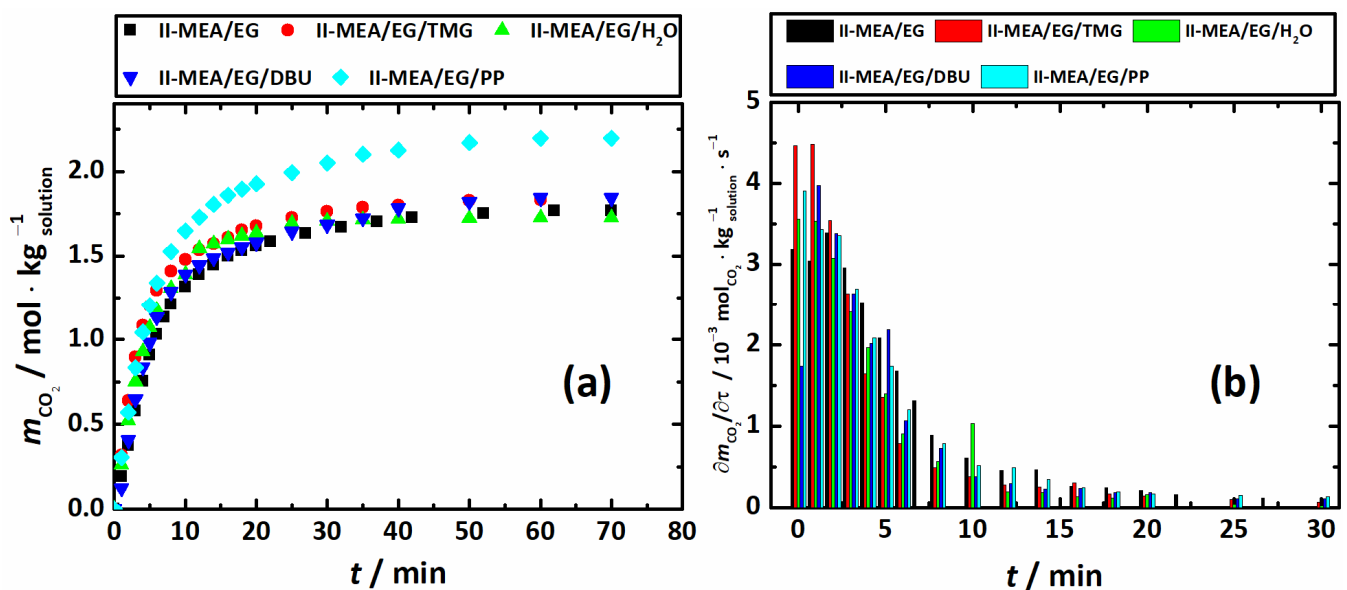


Figure 4. Absorption profiles (a) and absorption rates ($\partial m_{\text{CO}_2} / \partial \tau$) (b) of Series II systems, $T = 313.15$ K.

While the m_{CO_2} for the I-MEA/DMSO system is close to that of I-MEA/EG, I-MEA/H₂O demonstrates a 21% higher CO₂ absorption capacity. Obviously, from the point of view of the mass/moles of the absorbed gas, the system I-MEA/H₂O is the most promising within Series I. However, as discussed in the literature [23], H₂O-based amine solutions are rather volatile. When volatility is considered as an important parameter for the choice of the absorbing solution, the I-MEA/EG system is more attractive, despite showing a 17% lower absorption capacity compared to I-MEA/H₂O. Interestingly, the amine efficiency (c_{CO_2}) (Figure 5a) values of I-MEA/EG, I-DEA/EG, and I-MEA/H₂O are the same, within the error of estimation. For I-MEA/DMSO, the c_{CO_2} is approximately 10% higher, which indicates a favorable contribution of DMSO to amine efficiency. The EDA-based system (I-EDA/EG) shows m_{CO_2} and c_{CO_2} values that are almost 40% higher in comparison with I-MEA/EG. Indeed, this finding is in good agreement with the data from the literature [72,73]. The absorption rate for I-EDA/EG reaches 95% of its maximum in only 10 min. Certainly, these characteristics make the I-EDA/EG mixture the most promising among the studied

systems for efficient CO₂ capture. However, in the CO₂-saturated I-EDA/EG sample, a precipitate is formed, which results in full solution solidification. Thus, despite the good absorption properties of the EG-based mixture containing EDA, its practical applicability is quite doubtful.

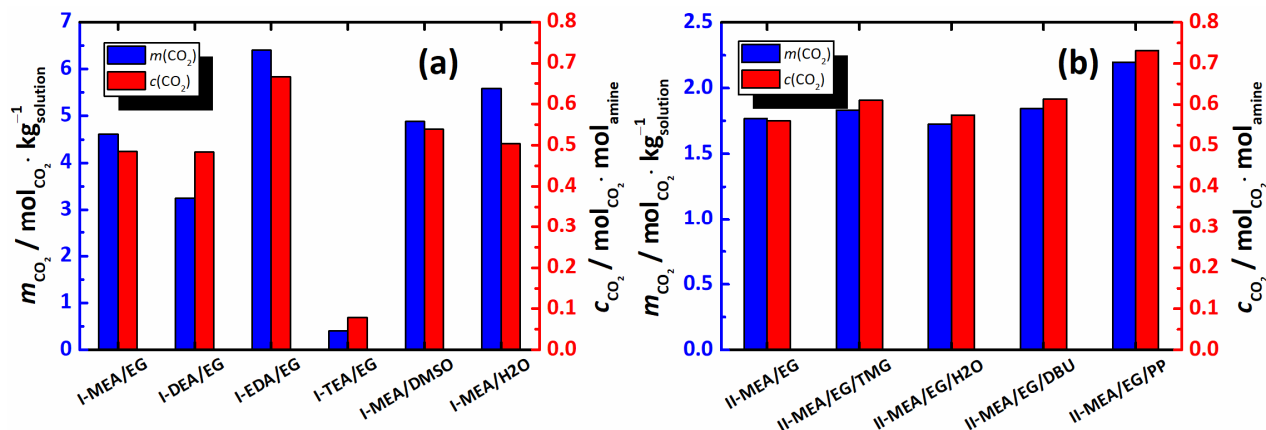


Figure 5. CO₂ absorption capacity (m_{CO_2} , blue) and MEA efficiency (c_{CO_2} , red) obtained for the mixtures of Series I (a) and II (b) at $T = 313.15$ K.

Figure 4a,b display absorption profiles and absorption rates ($\partial m_{\text{CO}_2} / \partial \tau$), respectively, for Series II systems, i.e., the neat mixture MEA/EG/ChCl with $x_1 = 0.222$, $x_2 = 0.667$, and $x_3 = 0.111$ (II-MEA/EG), and mixture II-MEA/EG containing 5 wt. % of promoters. Figure 5 shows the corresponding CO₂ absorption capacities (m_{CO_2}) and amine efficiency (c_{CO_2}).

As seen in Figure 4a,b, all the studied systems of Series II achieved 95% of their maximum absorption capacity in approximately 30 min. In principle, the absorption profiles can be conditionally divided into three time intervals. Within the first interval (<3 min), the highest CO₂ absorption rate is observed for the system containing water, II-MEA/EG/H₂O. Obviously, this is a viscosity-induced absorption rate increase, as the II-MEA/EG/H₂O mixture has the lowest viscosity in Series II. In approximately 3 min, the $\partial m_{\text{CO}_2} / \partial \tau$ of II-MEA/EG/H₂O drops significantly, and in the intermediate time interval (from 3 to 20 min), the rest of the Series II mixtures show higher $\partial m_{\text{CO}_2} / \partial \tau$ values than II-MEA/EG/H₂O. On average, within the second time interval, the neat mixture of MEA/EG/ChCl (system II-MEA/EG) shows the highest CO₂ absorption rate. The third interval (>20 min) is characterized by rather low $\partial m_{\text{CO}_2} / \partial \tau$ values, which, within the errors of estimation, are the same for all mixtures of Series II. The comparison of the results shown in Figure 4a,b enables us to conclude that, in general, the CO₂ absorption rate has no effect on the overall absorption capacity. As seen in Figure 5a,b, in the presence of the promoters, the absorption capacities increase in the order II-MEA/EG/PP > II-MEA/EG/DBU \approx II-MEA/EG/TMG > II-MEA/EG > II-MEA/EG/H₂O. However, on the whole, the positive contributions of TMG, DBU and PP to the CO₂ absorption capacity of II-MEA/EG are 4%, 9% and 30%, respectively, and the MEA efficiency increases by 30% for the latter system. Interestingly, when considering the overall process, H₂O has a negative effect on the CO₂ absorption of the MEA/EG/ChCl mixture. Clearly, the above order cannot be explained by the amounts of promoters added, as even when converted into mole fraction units, their concentrations decrease in the order H₂O > PP > TMG > DBU. Therefore, the most likely cause of this order is a difference in the mechanism of the reaction active in the chemical absorption of carbon dioxide by MEA, as promoted by the additives. Thus, in summing up the obtained results, it should be noted that from the point of view of the practical application of the investigated systems, PP represents the most promising promoter of CO₂ absorption, with only minor effects on the physical properties of the MEA/EG/ChCl mixtures.

4. Conclusions

In the present contribution, we outline the densities (ρ), viscosities (η) and absorption characteristics related to carbon dioxide for systems comprising amine (1), molecular solvent (MS, 2) and choline chloride (ChCl, 3), within the temperature range of $T = 278.15\text{--}363.15\text{ K}$ for physical properties, and at 313.15 K for CO_2 absorption capacity. The first part of the research includes an investigation of the effect of the mixture's composition, revealed by varying the amine from primary (monoethanolamine, MEA) to secondary (diethanolamine, DEA) and tertiary (triethanolamine, TEA), and by varying the degree of its substitution from mono- (MEA, DEA and TEA) to double-substituted (ethylenediamine, EDA) compounds. We also studied the role of an MS by exchanging ethylene glycol (EG) for water and dimethylsulfoxide (DMSO). As a base, a system with mole fractions of $x_1 = 0.667$, $x_2 = 0.222$, and $x_3 = 0.111$ was chosen. As was shown earlier [52], for this mixture composition, the CO_2 absorption parameters found for the MEA/EG/ChCl system show an optimal combination of absorbing capacity, m_{CO_2} , expressed in moles of CO_2 absorbed by 1 kg of a solution, and MEA efficiency, c_{CO_2} , moles of CO_2 absorbed by 1 mole of amine.

We show that when varying the amine in the amine/EG/ChCl mixtures, the ρ and η changes are determined by the properties of neat amines. This suggests that the natures of the interspecies interactions in these mixtures are very similar to that of the previously studied MEA/EG/ChCl system, namely, ChCl has a structure-breaking effect on the mixed amine/EG solvent, in which packing effects dominate over H-bonding interactions. When EG is exchanged for H_2O or DMSO, a decrease in density and an increase in viscosity are observed. A comparison of the data with the corresponding properties of pure MSs and the systems composed of each pair of the mixtures' components indicates that the intensity and/or number of interspecies interactions in the present ternary mixtures are stronger than those in pure H_2O , DMSO and MEA. For the corresponding CO_2 -saturated samples, the ρ and η increase proportionally to the amount of gas absorbed. The CO_2 absorption capacity of the EG-based mixtures decreases when going from primary to secondary and tertiary amines, and is 21% higher for the MEA/ H_2O /ChCl system compared to the mixtures containing EG and DMSO, which, in turn, show similar m_{CO_2} values.

The second part comprised an investigation of the presence of CO_2 absorption promoters in 5 wt. % of the MEA/EG/ChCl system, with mole fractions of $x_1 = 0.222$, $x_2 = 0.667$, and $x_3 = 0.111$, with which the best MEA efficiency was obtained [52]. As the promoters, N,N,N',N' -tetramethylguanidine, 1,8-diazabicyclo[5.4.0]undec-7-ene, 1,4-diazacyclohexane and water were used. We show that the addition of the promoters did not greatly affect the physical properties of the neat MEA/EG/ChCl mixture, while for the CO_2 -saturated samples, again, the higher the absorption capacity, the greater the increase in ρ and η . As shown, the greatest increase was observed for the piperazine-containing system, which was found to exhibit the highest CO_2 absorption capacity.

Supplementary Materials: The following supporting information can be downloaded at: <https://www.mdpi.com/article/10.3390/environments10050088/s1>. Tabulated density and viscosity before and after absorption of CO_2 , additional experimental data, including validation experiments, remaining water content, tabulated absorbing capacity (m_{CO_2}) and amine efficiency (c_{CO_2}).

Author Contributions: O.V.K.: data curation, writing—original draft, supervision, project administration, funding acquisition. A.A.G.: methodology, investigation, validation. Z.A.M.: formal analysis, investigation. A.N.P.: conceptualization, writing—review and editing. A.S.K.: methodology, investigation, writing—review and editing. A.A.A.: investigation, software. T.S.S.: formal analysis. A.N.M.: formal analysis, visualization. A.A.K.: formal analysis. A.V.B.: software, formal analysis. S.S.S.: validation, data curation. E.S.D.: investigation. I.V.V.: resources. A.V.V.: methodology, supervision. All authors have read and agreed to the published version of the manuscript.

Funding: This research was funded by Russian Science Foundation, grant number 21-73-00167.

Data Availability Statement: The authors confirm that the data supporting the findings of this study are available within the article and its Supplementary Materials.

Conflicts of Interest: The authors declare no conflict of interest.

References

- Wang, X.; Song, C. Carbon Capture From Flue Gas and the Atmosphere: A Perspective. *Front. Energy Res.* **2020**, *8*, 265. [\[CrossRef\]](#)
- Sanz-Pérez, E.S.; Murdock, C.R.; Didas, S.A.; Jones, C.W. Direct Capture of CO₂ from Ambient Air. *Chem. Rev.* **2016**, *116*, 11840–11876. [\[CrossRef\]](#)
- Metz, B.; Davidson, O.; De Coninck, H.C.; Loos, M.; Meyer, L. *IPCC Special Report on Carbon Dioxide Capture and Storage*; Cambridge University Press: Cambridge, UK, 2005; ISBN 0521685516.
- Ghanbari, T.; Abnisa, F.; Wan Daud, W.M.A. A Review on Production of Metal Organic Frameworks (MOF) for CO₂ Adsorption. *Sci. Total Environ.* **2020**, *707*, 135090. [\[CrossRef\]](#) [\[PubMed\]](#)
- Zhenhong, B.A.N.; Kokkeong, L.A.U.; Mohdshariff, A. Physical Absorption of CO₂ Capture: A Review. *Adv. Mater. Res.* **2014**, *917*, 134–143. [\[CrossRef\]](#)
- Abd, A.A.; Naji, S.Z.; Hashim, A.S.; Othman, M.R. Carbon Dioxide Removal through Physical Adsorption Using Carbonaceous and Non-Carbonaceous Adsorbents: A Review. *J. Environ. Chem. Eng.* **2020**, *8*, 104142. [\[CrossRef\]](#)
- Kazarina, O.V.; Petukhov, A.N.; Vorotyntsev, A.V.; Atlaskina, M.E.; Atlaskin, A.A.; Kazarin, A.S.; Golovacheva, A.A.; Sedova, N.A.; Markov, A.N.; Suvorov, S.S.; et al. The Way for Improving the Efficiency of Ammonia and Carbon Dioxide Absorption of Choline Chloride: Urea Mixtures by Modifying a Choline Cation. *Fluid Phase Equilib.* **2023**, *568*, 113736. [\[CrossRef\]](#)
- Kazarina, O.V.; Petukhov, A.N.; Nagrimanov, R.N.; Vorotyntsev, A.V.; Atlaskina, M.E.; Atlaskin, A.A.; Kazarin, A.S.; Golovacheva, A.A.; Markin, Z.A.; Markov, A.N.; et al. The Role of HBA Structure of Deep Eutectic Solvents Consisted of Ethylene Glycol and Chlorides of a Choline Family for Improving the Ammonia Capture Performance. *J. Mol. Liq.* **2023**, *373*, 121216. [\[CrossRef\]](#)
- Kazarina, O.V.; Agieienko, V.N.; Petukhov, A.N.; Vorotyntsev, A.V.; Atlaskina, M.E.; Atlaskin, A.A.; Kryuchkov, S.S.; Markov, A.N.; Nyuchev, A.V.; Vorotyntsev, I.V. Deep Eutectic Solvents Composed of Urea and New Salts of a Choline Family for Efficient Ammonia Absorption. *J. Chem. Eng. Data* **2022**, *67*, 138–150. [\[CrossRef\]](#)
- Kazarina, O.V.; Agieienko, V.N.; Nagrimanov, R.N.; Atlaskina, M.E.; Petukhov, A.N.; Moskvichev, A.A.; Nyuchev, A.V.; Barykin, A.V.; Vorotyntsev, I.V. A Rational Synthetic Approach for Producing Quaternary Ammonium Halides and Physical Properties of the Room Temperature Ionic Liquids Obtained by This Way. *J. Mol. Liq.* **2021**, *344*, 117925. [\[CrossRef\]](#)
- Yu, C.; Huang, C.; Tan, C. A Review of CO₂ Capture by Absorption and Adsorption. *Aerosol Air Qual. Res.* **2012**, *12*, 745–769. [\[CrossRef\]](#)
- Atlaskina, M.E.; Atlaskin, A.A.; Kazarina, O.V.; Petukhov, A.N.; Zarubin, D.M.; Nyuchev, A.V.; Vorotyntsev, A.V.; Vorotyntsev, I.V. Synthesis and Comprehensive Study of Quaternary-Ammonium-Based Sorbents for Natural Gas Sweetening. *Environments* **2021**, *8*, 134. [\[CrossRef\]](#)
- Atlaskin, A.A.; Kryuchkov, S.S.; Smorodin, K.A.; Markov, A.N.; Kazarina, O.V.; Zarubin, D.M.; Atlaskina, M.E.; Vorotyntsev, A.V.; Nyuchev, A.V.; Petukhov, A.N.; et al. Towards the Potential of Trihexyltetradecylphosphonium Indazolidine with Aprotic Heterocyclic Ionic Liquid as an Efficient Absorbent for Membrane-Assisted Gas Absorption Technique for Acid Gas Removal Applications. *Sep. Purif. Technol.* **2021**, *257*, 117835. [\[CrossRef\]](#)
- Borho, S.K.I.; Schmidt, J.J.M.S. Review: CO₂ Capturing Methods of the Last Two Decades. *Int. J. Environ. Sci. Technol.* **2022**. [\[CrossRef\]](#)
- Font-palma, C.; Cann, D.; Udemu, C. Review of Cryogenic Carbon Capture Innovations and Their Potential Applications. *C* **2021**, *7*, 58. [\[CrossRef\]](#)
- Hafeez, S.; Safdar, T.; Pallari, E.; Manos, G.; Aristodemou, E.; Zhang, Z. CO₂ Capture Using Membrane Contactors: A Systematic Literature Review. *Front. Chem. Sci. Eng.* **2021**, *15*, 720–754. [\[CrossRef\]](#)
- He, X. A Review of Material Development in the Field of Carbon Capture and the Application of Membrane-Based Processes in Power Plants and Energy-Intensive Industries. *Energy. Sustain. Soc.* **2018**, *8*, 34. [\[CrossRef\]](#)
- Vorotyntsev, I.V.; Atlaskin, A.A.; Trubyanov, M.M.; Petukhov, A.N.; Gumerova, O.R.; Akhmetshina, A.I.; Vorotyntsev, V.M. Towards the Potential of Absorbing Pervaporation Based on Ionic Liquids for Gas Mixture Separation. *Desalin. Water Treat.* **2017**, *75*, 305–313. [\[CrossRef\]](#)
- Abu-Zahra, M.R.M.; Schneiders, L.H.J.; Niederer, J.P.M.; Feron, P.H.M.; Versteeg, G.F. CO₂ Capture from Power Plants: Part I. A Parametric Study of the Technical Performance Based on Monoethanolamine. *Int. J. Greenh. Gas Control* **2007**, *1*, 37–46. [\[CrossRef\]](#)
- Luis, P. Use of Monoethanolamine (MEA) for CO₂ Capture in a Global Scenario: Consequences and Alternatives. *Desalination* **2016**, *380*, 93–99. [\[CrossRef\]](#)
- El Hadri, N.; Quang, D.V.; Goetheer, E.L.V.; Abu Zahra, M.R.M. Aqueous Amine Solution Characterization for Post-Combustion CO₂ Capture Process. *Appl. Energy* **2017**, *185*, 1433–1449. [\[CrossRef\]](#)
- Ko, Y.G.; Shin, S.S.; Choi, U.S. Primary, Secondary, and Tertiary Amines for CO₂ Capture: Designing for Mesoporous CO₂ Adsorbents. *J. Colloid Interface Sci.* **2011**, *361*, 594–602. [\[CrossRef\]](#) [\[PubMed\]](#)
- Cui, D.; Yan, S.; Guo, X.; Chu, F. Advance in Post-Combustion CO₂ Capture with Alkaline Solution: A Brief Review. *Energy Procedia* **2012**, *14*, 1515–1522. [\[CrossRef\]](#)
- Puxty, G.; Rowland, R.; Allport, A.; Yang, Q.; Bown, M.; Burns, R.; Maeder, M.; Attalla, M. Carbon Dioxide Postcombustion Capture: A Novel Screening Study of the Carbon Dioxide Absorption Performance of 76 Amines. *Environ. Sci. Technol.* **2009**, *43*, 6427–6433. [\[CrossRef\]](#) [\[PubMed\]](#)

25. Chowdhury, F.A.; Yamada, H.; Higashii, T.; Goto, K.; Onoda, M. CO₂ Capture by Tertiary Amine Absorbents: A Performance Comparison Study. *Ind. Eng. Chem. Res.* **2013**, *52*, 8323–8331. [\[CrossRef\]](#)
26. Leites, I.L. Thermodynamics of CO₂ Solubility in Mixtures Monoethanolamine with Organic Solvents and Water and Commercial Experience of Energy Saving Gas Purification Technology. *Energy Convers. Manag.* **1998**, *39*, 1665–1674. [\[CrossRef\]](#)
27. Barzagli, F.; Lai, S.; Mani, F.; Stoppioni, P. Novel Non-Aqueous Amine Solvents for Biogas Upgrading. *Energy Fuels* **2014**, *28*, 5252–5258. [\[CrossRef\]](#)
28. Zhang, J.; Misch, R.; Tan, Y.; Agar, D.W. Novel Thermomorphic Biphasic Amine Solvents for CO₂ Absorption and Low-Temperature Extractive Regeneration. *Chem. Eng. Technol.* **2011**, *34*, 1481–1489. [\[CrossRef\]](#)
29. Heldebrant, D.J.; Koech, P.K.; Glezakou, V.A.; Rousseau, R.; Malhotra, D.; Cantu, D.C. Water-Lean Solvents for Post-Combustion CO₂ Capture: Fundamentals, Uncertainties, Opportunities, and Outlook. *Chem. Rev.* **2017**, *117*, 9594–9624. [\[CrossRef\]](#)
30. Bougie, F.; Pokras, D.; Fan, X. Novel Non-Aqueous MEA Solutions for CO₂ Capture. *Int. J. Greenh. Gas Control* **2019**, *86*, 34–42. [\[CrossRef\]](#)
31. Hwang, K.S.; Park, S.W.; Park, D.W.; Oh, K.J.; Kim, S.S. Absorption of Carbon Dioxide into Diisopropanolamine Solutions of Polar Organic Solvents. *J. Taiwan Inst. Chem. Eng.* **2010**, *41*, 16–21. [\[CrossRef\]](#)
32. Kang, M.K.; Jeon, S.B.; Cho, J.H.; Kim, J.S.; Oh, K.J. Characterization and Comparison of the CO₂ Absorption Performance into Aqueous, Quasi-Aqueous and Non-Aqueous MEA Solutions. *Int. J. Greenh. Gas Control* **2017**, *63*, 281–288. [\[CrossRef\]](#)
33. Chen, S.; Chen, S.; Fei, X.; Zhang, Y.; Qin, L. Solubility and Characterization of CO₂ in 40 Mass % N-Ethylmonoethanolamine Solutions: Explorations for an Efficient Nonaqueous Solution. *Ind. Eng. Chem. Res.* **2015**, *54*, 7212–7218. [\[CrossRef\]](#)
34. Barbarossa, V.; Barzagli, F.; Mani, F.; Lai, S.; Stoppioni, P.; Vanga, G. Efficient CO₂ Capture by Non-Aqueous 2-Amino-2-Methyl-1-Propanol (AMP) and Low Temperature Solvent Regeneration. *RSC Adv.* **2013**, *3*, 12349–12355. [\[CrossRef\]](#)
35. Bihong, L.; Kexuan, Y.; Xiaobin, Z.; Zuoming, Z.; Guohua, J. 2-Amino-2-Methyl-1-Propanol Based Non-Aqueous Absorbent for Energy-Efficient and Non-Corrosive Carbon Dioxide Capture. *Appl. Energy* **2020**, *264*, 114703. [\[CrossRef\]](#)
36. Guo, H.; Li, C.; Shi, X.; Li, H.; Shen, S. Nonaqueous Amine-Based Absorbents for Energy Efficient CO₂ Capture. *Appl. Energy* **2019**, *239*, 725–734. [\[CrossRef\]](#)
37. Kollau, L.J.B.M.; Vis, M.; Van Den Bruinhorst, A.; Esteves, A.C.C.; Tuinier, R. Quantification of the Liquid Window of Deep Eutectic Solvents. *Chem. Commun.* **2018**, *54*, 13351–13354. [\[CrossRef\]](#)
38. Kovács, A.; Neyts, E.C.; Cornet, I.; Wijnants, M.; Billen, P. Modeling the Physicochemical Properties of Natural Deep Eutectic Solvents. *ChemSusChem* **2020**, *13*, 3789–3804. [\[CrossRef\]](#)
39. Amoroso, R.; Hollmann, F.; Maccallini, C. Choline Chloride-Based DES as Solvents/Catalysts/Chemical Donors in Pharmaceutical Synthesis. *Molecules* **2021**, *26*, 6286. [\[CrossRef\]](#)
40. Mannu, A.; Cardano, F.; Fin, A.; Baldino, S.; Prandi, C. Choline Chloride-Based Ternary Deep Band Gap Systems. *J. Mol. Liq.* **2021**, *330*, 115717. [\[CrossRef\]](#)
41. Mannu, A.; Cardano, F.; Baldino, S.; Fin, A. Behavior of Ternary Mixtures of Hydrogen Bond Acceptors and Donors in Terms of Band Gap Energies. *Materials* **2021**, *14*, 3418. [\[CrossRef\]](#)
42. Hansen, B.B.; Spittle, S.; Chen, B.; Poe, D.; Zhang, Y.; Klein, J.M.; Horton, A.; Adhikari, L.; Zelovich, T.; Doherty, B.W.; et al. Deep Eutectic Solvents: A Review of Fundamentals and Applications. *Chem. Rev.* **2021**, *121*, 1232–1285. [\[CrossRef\]](#) [\[PubMed\]](#)
43. Pelaquim, F.P.; Barbosa Neto, A.M.; Dalmolin, I.A.L.; Costa, M.C. da Gas Solubility Using Deep Eutectic Solvents: Review and Analysis. *Ind. Eng. Chem. Res.* **2021**, *60*, 8607–8620. [\[CrossRef\]](#)
44. Marcus, Y. Gas Solubilities in Deep Eutectic Solvents. *Monatshefte für Chemie* **2018**, *149*, 211–217. [\[CrossRef\]](#)
45. Fourmentin, S.; Gomes, M.C. *Deep Eutectic Solvents for Medicine, Gas Solubilization and Extraction of Natural Substances*; Lichtfouse, E., Fourmentin, S., Gomes, M.C., Eds.; Springer Nature Switzerland AG: Cham, Switzerland, 2021; ISBN 978-3-030-53068-6.
46. Mahi, M.R.; Mokbel, I.; Négadi, L.; Jose, J. CO₂ Capture Using Deep Eutectic Solvent and Amine (MEA) Solution. In *Cutting Edge for Carbon Capture Utilization and Storage*; Wiley: New York, NY, USA, 2017; pp. 309–316. ISBN 9781119363804.
47. Adeyemi, I.; Abu-Zahra, M.R.M.; Alnashef, I. Experimental Study of the Solubility of CO₂ in Novel Amine Based Deep Eutectic Solvents. *Energy Procedia* **2017**, *105*, 1394–1400. [\[CrossRef\]](#)
48. Li, Z.; Wang, L.; Li, C.; Cui, Y.; Li, S.; Yang, G.; Shen, Y. Absorption of Carbon Dioxide Using Ethanolamine-Based Deep Eutectic Solvents. *ACS Sustain. Chem. Eng.* **2019**, *7*, 10403–10414. [\[CrossRef\]](#)
49. Pasha, M.; Zhang, H.; Shang, M.; Li, G.; Su, Y. CO₂ Absorption with Diamine Functionalized Deep Eutectic Solvents in Microstructured Reactors. *Process Saf. Environ. Prot.* **2022**, *159*, 106–119. [\[CrossRef\]](#)
50. Cheng, J.; Wu, C.; Gao, W.; Li, H.; Ma, Y.; Liu, S.; Yang, D. CO₂ Absorption Mechanism by the Deep Eutectic Solvents Formed by Monoethanolamine-Based Protic Ionic Liquid and Ethylene Glycol. *Int. J. Mol. Sci.* **2022**, *23*, 1893. [\[CrossRef\]](#)
51. Zhang, N.; Huang, Z.; Zhang, H.; Ma, J.; Jiang, B.; Zhang, L. Highly Efficient and Reversible CO₂ Capture by Task-Specific Deep Eutectic Solvents. *Ind. Eng. Chem. Res.* **2019**, *58*, 13321–13329. [\[CrossRef\]](#)
52. Kazarina, O.V.; Agieienko, V.N.; Petukhov, A.N.; Vorotyntsev, A.V.; Kazarin, A.S.; Atlaskina, M.E.; Atlaskin, A.A.; Markov, A.N.; Golovacheva, A.A.; Vorotyntsev, I. V Monoethanolamine + Ethylene Glycol + Choline Chloride: An Effect of the Mixture Composition on the CO₂ Absorption Capacity, Density and Viscosity. *J. Chem. Eng. Data* **2022**, *67*, 2899–2912. [\[CrossRef\]](#)
53. Bhawna; Pandey, A.; Pandey, S. Superbase-Added Choline Chloride-Based Deep Eutectic Solvents for CO₂ Capture and Sequestration. *ChemistrySelect* **2017**, *2*, 11422–11430. [\[CrossRef\]](#)

54. Fu, H.; Hou, Y.; Sang, H.; Mu, T.; Lin, X.; Peng, Z.; Li, P.; Liu, J. Carbon Dioxide Capture by New DBU-Based DES: The Relationship between Ionicity and Absorptive Capacity. *AIChE J.* **2021**, *67*, e17244. [[CrossRef](#)]
55. Jiang, B.; Ma, J.; Yang, N.; Huang, Z.; Zhang, N.; Tantai, X.; Sun, Y.; Zhang, L. Superbase/Acylamido-Based Deep Eutectic Solvents for Multiple-Site Efficient CO₂ Absorption. *Energy and Fuels* **2019**, *33*, 7569–7577. [[CrossRef](#)]
56. Yan, H.; Zhao, L.; Bai, Y.; Li, F.; Dong, H.; Wang, H.; Zhang, X.; Zeng, S. Superbase Ionic Liquid-Based Deep Eutectic Solvents for Improving CO₂ Absorption. *ACS Sustain. Chem. Eng.* **2020**, *8*, 2523–2530. [[CrossRef](#)]
57. Chirico, R.D.; Frenkel, M.; Magee, J.W.; Diky, V.; Muzny, C.D.; Kazakov, A.F.; Kroenlein, K.; Abdulagatov, I.; Hardin, G.R.; Acree, W.E.; et al. Improvement of Quality in Publication of Experimental Thermophysical Property Data: Challenges, Assessment Tools, Global Implementation, and Online Support. *J. Chem. Eng. Data* **2013**, *58*, 2699–2716. [[CrossRef](#)]
58. Huertas, J.I.; Gomez, M.D.; Giraldo, N.; Garzón, J. CO₂ Absorbing Capacity of MEA. *J. Chem.* **2015**, *2015*, 965015. [[CrossRef](#)]
59. Deng, D.; Gao, B.; Zhang, C.; Duan, X.; Cui, Y.; Ning, J. Investigation of Protic NH₄SCN-Based Deep Eutectic Solvents as Highly Efficient and Reversible NH₃ Absorbents. *Chem. Eng. J.* **2019**, *358*, 936–943. [[CrossRef](#)]
60. Li, K.; Fang, H.; Duan, X.; Deng, D. Efficient Uptake of NH₃ by Dual Active Sites NH₄SCN-Imidazole Deep Eutectic Solvents with Low Viscosity. *J. Mol. Liq.* **2021**, *339*, 116724. [[CrossRef](#)]
61. Lee, J.I.; Otto, F.D.; Mather, A.E. Equilibrium Between Carbon Dioxide and Aqueous Monoethanolamine Solutions. *J. Appl. Chem. Biotechnol.* **1976**, *26*, 541–549. [[CrossRef](#)]
62. Jou, F.-Y.; Mather, A.E.; Otto, F.D. The Solubility of CO₂ in a 30 Mass Percent Monoethanolamine Solution. *Can. J. Chem. Eng.* **1995**, *73*, 140–147. [[CrossRef](#)]
63. Shen, K.P.; Li, M.H. Solubility of Carbon Dioxide in Aqueous Mixtures of Monoethanolamine with Methyldiethanolamine. *J. Chem. Eng. Data* **1992**, *37*, 96–100. [[CrossRef](#)]
64. Shaukat, S.; Buchner, R. Densities, Viscosities [from (278.15 to 318.15) K], and Electrical Conductivities (at 298.15 K) of Aqueous Solutions of Choline Chloride and Chloro-Choline Chloride. *J. Chem. Eng. Data* **2011**, *56*, 4944–4949. [[CrossRef](#)]
65. Hawrylak, B.; Burke, S.E.; Palepu, R. Partial Molar and Excess Volumes and Adiabatic Compressibilities of Binary Mixtures of Ethanolamines with Water. *J. Solution Chem.* **2000**, *29*, 575–594. [[CrossRef](#)]
66. Mjalli, F.S.; Murshid, G.; Al-Zakwani, S.; Hayyan, A. Monoethanolamine-Based Deep Eutectic Solvents, Their Synthesis and Characterization. *Fluid Phase Equilib.* **2017**, *448*, 30–40. [[CrossRef](#)]
67. Agieienko, V.; Buchner, R. A Comprehensive Study of Density, Viscosity, and Electrical Conductivity of (Choline Chloride + Glycerol) Deep Eutectic Solvent and Its Mixtures with Dimethyl Sulfoxide. *J. Chem. Eng. Data* **2021**, *66*, 780–792. [[CrossRef](#)]
68. Wang, X.; Yang, F.; Gao, Y.; Liu, Z. Volumetric Properties of Binary Mixtures of Dimethyl Sulfoxide with Amines from (293.15 to 363.15) K. *J. Chem. Thermodyn.* **2013**, *57*, 145–151. [[CrossRef](#)]
69. Choi, J.H.; Oh, S.G.; Kim, Y.E.; Yoon, Y.I.; Nam, S.C. Carbon Dioxide Absorption Characteristics of Aqueous Alkanolamine Using Nuclear Magnetic Resonance Spectroscopy. *Environ. Eng. Sci.* **2012**, *29*, 328–334. [[CrossRef](#)]
70. Gonzalez-Garza, D.; Rivera-Tinoco, R.; Bouallou, C. Comparison of Ammonia, Monoethanolamine, Diethanolamine and Methyldiethanolamine Solvents to Reduce CO₂ Greenhouse Gas Emissions. *Chem. Eng. Trans.* **2009**, *18*, 279–284. [[CrossRef](#)]
71. Liu, X.; Ao, Q.; Shi, S.; Li, S. CO₂ Capture by Alcohol Ammonia Based Deep Eutectic Solvents with Different Water Content. *Mater. Res. Express* **2022**, *9*, 015504. [[CrossRef](#)]
72. Zhou, S.; Chen, X.; Nguyen, T.; Voice, A.K.; Rochelle, G.T. Aqueous Ethylenediamine for CO₂ Capture. *ChemSusChem* **2010**, *3*, 913–918. [[CrossRef](#)]
73. Tao, M.; Gao, J.; Zhang, P.; Zhang, W.; Liu, Q.; He, Y.; Shi, Y. Biogas Upgrading by Capturing CO₂ in Non-Aqueous Phase-Changing Diamine Solutions. *Energy Fuels* **2017**, *31*, 6298–6304. [[CrossRef](#)]

Disclaimer/Publisher's Note: The statements, opinions and data contained in all publications are solely those of the individual author(s) and contributor(s) and not of MDPI and/or the editor(s). MDPI and/or the editor(s) disclaim responsibility for any injury to people or property resulting from any ideas, methods, instructions or products referred to in the content.